IGF-I mRNA and Signaling in the Diabetic Retina

Chiara Gerhardinger, Kimberly D. McClure, Giulio Romeo, Francesca Podestà, and Mara Lorenzi

IGF-I promotes the survival of multiple cell types by activating the IGF-I receptor (IGF-IR), which signals downstream to a serine/threonine kinase termed Akt. Because in diabetes vascular and neural cells of the retina undergo accelerated apoptosis, we examined IGF-I synthesis and signaling in the human and rat diabetic retina. In retinas obtained postmortem from six donors aged 64 ± 8 years with a diabetes duration of 7 ± 5 years, IGF-I mRNA levels were threefold lower than in the retinas of six age-matched nondiabetic donors ($P = 0.005$). In the retinas of rats with 2 months' duration of streptozotocin-induced diabetes, IGF-I mRNA levels were similar to those of control rats, but after 5 months of diabetes they failed to increase to the levels recorded in age-matched controls ($P < 0.02$). Retinal IGF-I expression was not altered by hypophysectomy, proving to be growth-hormone independent. IGF-IR levels were modestly increased in the human diabetic retinas ($P = 0.02$ vs. nondiabetic retinas) and were unchanged in the diabetic rats. Phosphorylation of the IGF-IR could be measured only in the rat retina, and was not decreased in the diabetic rats (94 ± 18% of control values). In the same diabetic rats, phosphorylation of Akt was 123 ± 21% of control values. There was not yet evidence of increased apoptosis of retinal microvascular cells after 5 months of streptozotocin-induced diabetes. Hence, in the retina of diabetic rats, as in the retina of diabetic human donors, IGF-I mRNA levels are substantially lower than in age-matched nondiabetic controls, whereas IGF-IR activation and signaling are not affected, at least for some time. This finding suggests that in the diabetic retina, the activation of the IGF-IR is modulated by influences that compensate for, or are compensated by, decreased IGF-I synthesis. *Diabetes* 50:175–183, 2001

There is growing evidence that diabetes induces an apoptogenic environment in the retina. In both human and experimental diabetes, pericytes and endothelial cells of the retinal capillaries manifest morphological and molecular features of apoptosis, before the appearance of histological lesions (1). Pericytes isolated from the retina of diabetic eye donors show overexpression of CPP32, a member of the family of interleukin-1β–converting enzymes with caspase activity (2). Pericytes studied in situ in human diabetic retinas show increased levels of Bax—a death-inducing member of the Bcl-2 family—often in association with fragmented chromatin (3). Bax is also expressed by retinal ganglion cells and cells of the inner nuclear layer, and its levels are increased in preparations of the whole human diabetic retina (3). Neural cells of the inner retina manifest signs of apoptosis in human and experimental diabetes, even in the absence of retinal microangiopathy (4).

The preferential, if not exclusive, occurrence of diabetes-induced apoptosis in the nonphotoreceptor regions of the retina—consistent with the clinical manifestations of diabetic retinopathy—suggests a causative or permissive role for events taking place in the inner retina. Decreased signaling by the growth/survival factor IGF-I is a prominent candidate for several reasons. Both IGF-I and its receptor (IGF-IR) are expressed in the inner retina (5,6), and retinal microvascular cells produce (7) and respond to (8) IGF-I in vitro. Activation of the IGF-IR exerts powerful antiapoptotic effects, protecting multiple cell types against a variety of death signals (9). Central to the prosurvival action of IGF-I is the phosphorylation of Akt/protein kinase B, occurring through the sequential steps of IGF-IR–mediated activation of insulin receptor substrate-1, in turn activating phosphatidylinositol 3-kinase, which activates Akt (9,10). Akt promotes cell survival through phosphorylation of several substrates: BAD—a member of the Bcl-2 family—which becomes unable to heterodimerize with, and thus inactivate, prosurvival Bcl-X_L (9); caspase 9, which loses protease activity (11); and members of the Forkhead family of transcription factors, which are prevented from translocating to the nucleus and activating proapoptotic genes (10). Of note, neuronal death by growth factor deprivation appears to require the presence of Bax (12).

In poorly controlled diabetes, IGF-I synthesis is decreased in several tissues and organs (13–16). No data pertaining to the human retina in the early stages of diabetes have been reported to our knowledge, and the data obtained in the rat retina are potentially conflicting. Lowe et al. (17) found a prominent decrease in retinal IGF-I mRNA levels after 3 weeks of streptozotocin-induced diabetes, while Charkrabarti et al. (18) reported no change from control values in BB/W rats with 3 months of diabetes. To establish whether a role can be entertained for decreased IGF-I signaling in the early retinal pathology caused by diabetes, we measured IGF-I mRNA and IGF-IR levels in the retina of eye donors with short diabetes duration as well as streptozotocin-induced diabetic rats. In the diabetic rats, we also examined the phosphorylation of the IGF-IR and Akt, and the occurrence of retinal capillary cell apoptosis. IGF-IR phosphorylation is the event that uniquely informs about IGF-I activity, since all downstream steps in the intracellular signal transduction pathway are in common with the insulin receptor (19). To gain insight into the mechanisms responsible for decreased IGF-I synthesis in

From the Schepens Eye Research Institute (C.G., K.D.M., G.R., F.P., M.L.) and the Department of Ophthalmology (C.G., G.R., F.P., M.L.), Harvard Medical School, Boston, Massachusetts.

Address correspondence and reprint requests to Mara Lorenzi, MD, Schepens Eye Research Institute, 20 Staniford St., Boston, MA 02114. E-mail: lorenzi@vision.eri.harvard.edu.

Received for publication 9 March 2000 and accepted in revised form 20 September 2000.

BSA, bovine serum albumin; C-RT-PCR, competitive reverse transcriptase–polymerase chain reaction; IGF-IR, IGF-I receptor; PCR, polymerase chain reaction; TBST, Tris-buffered saline containing 0.05% Tween-20; TUNEL, terminal deoxynucleotidyl transferase–mediated dUTP nick-end labeling.

TABLE 1
Primers used for PCR amplification of IGF-I and β-actin from rat tissues and for the synthesis of specific competitors

		Sequence (5′ → 3′)	Position	Accession #
IGF-I	Forward	GCATTGTGGATGAGTGTTGC	984–1,004	MI15481
	Reverse	GGTCTTGTTTCCTGCACTTC	1,165–1,146	
	Reverse hybrid	reverse + GTCTTGGGCATGTCAGTGTG	1,165–1,146 + 1,110–1,091	
β-actin	Forward	TTGTAACCAACTGGGACGATATGG	1,552–1,575	J00691
	Reverse	GATCTTGATCTTCATGGTGCTAGG	2,864–2,841	
	Reverse hybrid	reverse + GCACTGTGTTGGCATAGAGG	2,864–2,841 + 2,775–2,756	

The IGF-I and β-actin competitors were produced by RT-PCR of rat retinal RNA with the respective forward and reverse-hybrid primers. The conditions for IGF-I C-PCR were denaturation 1 min at 94°C, annealing 1 min at 58°C, and extension 1 min at 72°C for 25 cycles, yielding a 181-bp fragment corresponding to the endogenous IGF-Ia transcript, and a 146-bp fragment corresponding to the IGF-I competitor. The conditions for β-actin C-PCR were denaturation 1 min at 95°C, annealing 45 s at 60°C, and extension 1.5 min at 72°C for 22 cycles, yielding a 761-bp fragment corresponding to the endogenous β-actin transcript, and a 692-bp fragment corresponding to the β-actin competitor.

the diabetic retina, we investigated the growth-hormone dependency of retinal IGF-I, as well as IGF-I mRNA and signaling in rats with experimental galactosemia. These rats exhibit elevated blood hexose concentrations and develop retinal microvascular cell apoptosis and a diabetic-like retinopathy in the absence of altered insulin levels (20).

RESEARCH DESIGN AND METHODS

Human eyes and specimens. Human eyes were obtained from certified eye banks through the National Disease Research Interchange. Criteria for inclusion in the study were age <70 years, the fewest possible chronic pathologies other than diabetes, absence of retinal or hematological diseases and uremia, and absent administration of chemotherapy or life-support measures. Diabetes duration was <15 years to address mostly background retinopathy. The eyes of the diabetic and age-matched nondiabetic donors were enucleated 3 ± 2 and 3 ± 1 h after death, respectively. Eyes or poles were kept at 4°C by the eye bank, and shipped to the laboratory on ice; the time elapsed from death to processing was 28 ± 8 h for the diabetic specimens and 28 ± 6 h for the control specimens.

The eyes used for isolation of total retinal RNA were obtained from six diabetic donors (age 64 ± 8 years, diabetes duration 7 ± 5 years) and six nondiabetic donors (age 62 ± 7 years). The two retinas from each donor were immediately dissected, separated from the retinal pigmented epithelium, pooled, and homogenized in guanidine isothiocyanate. RNA was isolated by centrifugation on cesium chloride followed by ethanol precipitation.

The eyes used for preparation of retinal protein were obtained from 10 diabetic (age 66 ± 7 years, diabetes duration 8 ± 4 years) and 10 nondiabetic donors (age 66 ± 6 years). The dissected retinas were homogenized in ice-cold lysis buffer containing phosphatase and protease inhibitors (30 mmol/l Tris-HCl, pH 7.4, 10 mmol/l EGTA, 5 mmol/l EDTA, 250 mmol/l sucrose, 1% Triton-X-100, 1 mmol/l NaF, 1 mmol/l Na_3VO_4, 1 mmol/l phenylmethylsulfonyl fluoride, 5 μg/ml leupeptin, 5 μg/ml pepstatin, and 15 μg/ml aprotinin). The homogenate was sonicated three times for 2 s, centrifuged at 16,000*g* for 15 min at 4°C, and the supernatant was collected and stored in aliquots at –80°C. Protein concentration was determined with the Bradford method using bovine serum albumin (BSA) as standard (protein assay kit; Bio-Rad, Hercules, CA). Protein lysates were also prepared from human retinal microvessels isolated from the neural retina by osmotic lysis (3). Homogenates of human brain, heart, and kidney (Protein Medley) were purchased from Clontech (Palo Alto, CA).

Animals and specimens. Sprague-Dawley male rats (6 weeks old [Taconic Farms, Germantown, NY]) were randomly assigned to one of the following groups: normal, diabetic, or galactosemic. Diabetes was induced by intravenous administration of streptozotocin (55 mg/kg body wt, dissolved in citrate buffer, pH 4.5). Experimental galactosemia was induced by feeding regular rat diet containing 30% D-galactose (Sigma, St. Louis, MO). The animals were treated in conformity with the Association for Research in Vision and Ophthalmology resolution on treatment of animals in research. All rats had free access to food and water. Body weight was recorded twice weekly in the diabetic rats, and 1–2 U insulin (NPH insulin; Novo Nordisk, Princeton, NJ) was given subcutaneously as needed to avoid weight loss without preventing hyperglycemia and glycosuria. The last insulin injection was given 5.6 ± 3.6 days before the rats were killed. Whole blood for measurement of HbA_{1c} was obtained by intracardiac sampling at the time of killing. After 2 and 5 months of diabetes or galactose feeding, the animals were killed by CO_2 inhalation. The eyes were immediately removed, and the retinas were dissected under a microscope and processed for RNA or protein isolation as described above. The brain, heart, and kidneys were also excised and processed for protein isolation. The eyes of other rats were fixed in 10% buffered formalin, and the retinas were digested with trypsin (1) to isolate the vascular network.

Four normal rats were used to assess the postmortem stability of the IGF-I mRNA and IGF-IR. One eye of each rat was enucleated and processed at the time of sacrifice, the other eye was enucleated 3 h after sacrifice and kept at 4°C for an additional 24 h to match the timing of events reported above for the human specimens. The retinas were then isolated and processed for RNA and protein extraction.

Sprague-Dawley hypophysectomized and sham-operated control rats were obtained from Taconic Farms. The rats were killed 2 weeks after surgery, and the retina, brain, and liver were collected and processed for RNA isolation.

Northern blot analysis. Northern blot analysis was used to study the levels of IGF-I mRNA in human retinas, and was performed as described previously (21). Membranes were hybridized to a full-length human IGF-I cDNA probe (gift of Dr. Peter Rotwein) containing a 780-nucleotide fragment that is present in all types of IGF-I transcripts, and, to control for loading, to a 457-bp human β-actin cDNA (21). Probes were labeled using the Multiprime labeling kit (Amersham Pharmacia Biotech, Piscataway, NJ) and [^{32}P]dCTP. The hybridization signal was quantitated using a PhosphorImaging system (Molecular Dynamics, Sunnyvale, CA). Data are expressed as IGF-I–to–β-actin ratio. After quantitation, blots were exposed to Kodak AR films, and the autoradiographs used for photography.

Competitive reverse transcriptase–polymerase chain reaction. Competitive reverse transcriptase–polymerase chain reaction (C-RT-PCR) was used to study the levels of IGF-I mRNA in individual rat retinas because of the small amount of RNA available. Specific competitors for IGF-I and the housekeeping gene β-actin were synthesized by polymerase chain reaction (PCR) using hybrid reverse primers as described by Celi et al. (22). The 3′ half of the hybrid reverse primer corresponds to the sequence of the reverse primer, whereas the 5′ half corresponds to a sequence of the target transcript *n* nucleotides upstream from the reverse primer. Thus, PCR amplification with the forward primer for the transcript of interest in combination with the corresponding hybrid reverse primer will generate a competitor template identical to the endogenous product but for a deletion of *n* nucleotides. The primers and PCR conditions for IGF-I and β-actin are described in Table 1. A specific competitor for the housekeeping gene cyclophilin was obtained by RT-PCR of a cyclophilin-armored RNA competitor template containing a 25-bp internal deletion (RT Check kit; Ambion, Austin, TX). After amplification, the competitors were resolved by agarose gel electrophoresis, purified using the QIAEX II gel extraction system (Qiagen, Chatsworth, CA), diluted to 100 attomol/ml in TE buffer (10 mmol/l Tris-HCl, pH 7.5, 0.1 mmol/l EDTA) containing 10 mg/ml glycogen, and stored in aliquots at –80°C. The specificity of each PCR product was verified by size and restriction digestion.

Reverse transcriptions were carried out with 1 μg total RNA as described previously (21). Samples from an equal number of diabetic, galactosemic, and control retinas were always processed simultaneously. Equal volumes of each cDNA were added to three different known amounts of the specific competitor, and PCR amplification was performed with the cycle conditions described in Table 1. The PCR products were resolved by agarose gel electrophoresis (4 and 3% NuSieve; FMC Bioproducts, Rockland, ME, for IGF-I and β-actin, respectively, and 3% Metaphor; FMC Bioproducts, for cyclophilin), visualized with GelStar (FMC Bioproducts), and quantitated with the Bio-Rad Gel

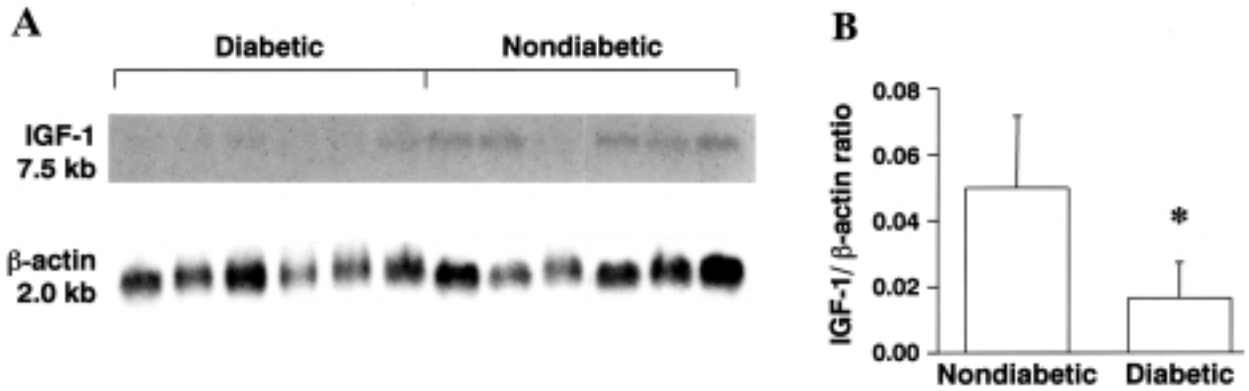

FIG. 1. IGF-I mRNA levels in the retina of diabetic and nondiabetic donors. Northern blots (15 µg total RNA per lane) were hybridized as described in RESEARCH DESIGN AND METHODS. *A*: Autoradiographs of IGF-I (5 days of exposure) and β-actin (20 h of exposure). *B*: IGF-I–to–β-actin ratios computed from phosphorimager quantitation of the IGF-I and β-actin mRNA signal. Bars represent the mean ± SD of the values obtained in the six diabetic and six nondiabetic donors studied. *P = 0.005.

Documentation System equipped with the QuantityOne software. The amount of the endogenous transcript in each retina was determined for each of the three competitor concentrations as follows: moles of endogenous = (intensity of endogenous/intensity of competitor) × moles of competitor. The three values for each sample were averaged and normalized for the amount of input RNA by dividing the average value by the corresponding value of the housekeeping gene determined in the same way. Because the accuracy of competitor concentration may not be absolute, the data are presented as transcript-to-housekeeping ratio.

The linearity of the PCRs and the appropriate concentration of competitors to be used were determined as described by Vafiadis et al. (23).

Immunoblotting and immunoprecipitation. The IGF-IR levels in human and rat retinas were determined by immunoblotting of retinal lysates performed as described previously (24). Proteins (50 µg) were resolved by electrophoresis on 7.5% SDS-PAGE. Each gel always included an equal number of samples from diabetic and nondiabetic human retinas, or diabetic, galactosemic, and control rat retinas. Proteins were transferred onto nitrocellulose membrane (Bio-Rad) by electroblotting using 25 mmol/l Tris, pH 8.3, 192 mmol/l glycine, 20% methanol buffer containing 0.1% SDS. After blocking overnight at 4°C in 10% nonfat milk in Tris-buffered saline containing 0.05% Tween-20 (TBST), the blots were probed with rabbit polyclonal antibodies against the α or β subunits of the IGF-IR (SantaCruz Biotechnology, Santa Cruz, CA), diluted in TBST, washed, and incubated with horseradish peroxidase–conjugated secondary antibodies. Immunoreactive bands were visualized by enhanced chemiluminescence (SuperSignal West Pico Chemiluminescent Substrate System; Pierce, Rockford, IL). Densitometric quantitation of the autoradiographs was performed with the model 330A computing densitometer (Molecular Dynamics). Data are expressed as densitometric units/micrograms of protein.

Tyrosine phosphorylation of the retinal IGF-IR was detected by immunoprecipitation followed by Western blot analysis. Equal amounts (200 µg) of solubilized protein obtained from individual retinas of diabetic, galactosemic, and control rats, respectively, were incubated in lysis buffer (described above for the homogenization of retinal samples) with anti–IGF-IR β-subunit antibody at 4°C overnight. Lysates of human skin fibroblasts treated with IGF-I (Sigma; 100 ng/ml in serum-free medium for 30 min) were used to positively identify the tyrosine-phosphorylated IGF-IR β-subunit. The immunocomplexes were precipitated by addition of protein-A sepharose (Sigma), and the resulting immunoprecipitates were washed four times with lysis buffer and resuspended by boiling in Laemmli sample buffer supplemented with β-mercaptoethanol. Proteins were resolved by SDS-PAGE and electroblotted onto nitrocellulose membranes. Blots were blocked in 4% BSA-TBST, and tyrosine-phosphorylated proteins were detected by immunoblotting with a mixture of antiphosphotyrosine monoclonal antibodies (clone PY20; Signal Transduction Laboratories, Lexington, KY, and clone 4G10; Upstate Biotechnology, Lake Placid, NY) both diluted 1:5,000. To control for the amount of immunoprecipitated IGF-IR, companion blots, blocked in 10% nonfat milk, were probed with the IGF-IR β-subunit antibodies. IGF-IR phosphorylation was computed as percentage of control, after normalization for the amount of immunoprecipitated IGF-IR.

The levels of Akt phosphorylation were studied by immunoblot using antibodies that detect Akt only when phosphorylated at Ser 473 (Phospho-Akt [Ser 473] Antibody; New England Biolabs, Beverly, MA). To control for the amount of Akt in each retina sample, companion blots were probed with Akt antibodies (New England Biolabs). Immunoreactive proteins were detected and quantitated as above, and Akt phosphorylation was computed as percentage of control, after normalization for the amount of total Akt.

Analysis of DNA fragmentation in retinal vessels. Microvascular cell apoptosis in rat retinal trypsin digests was studied with the terminal deoxynucleotidyl transferase–mediated dUTP nick-end labeling (TUNEL) assay using the In Situ Cell Death Detection Kit by Boehringer Mannheim Biochemicals (Indianapolis, IN) (1). TUNEL-positive nuclei were examined for chromatin fragmentation and/or presence of apoptotic bodies, and attributed to specific microvascular cells as described previously (1).

Statistical analysis. The data are summarized with the mean ± SD. Statistical analysis was performed with the unpaired t test in the human study and the hypophysectomized rat study; analysis of variance, followed by the Fisher's multiple comparison test, was used for all other rat studies. Linear regression was used to test correlations.

RESULTS

IGF-I expression is decreased in both human and rat diabetic retinas. Northern analysis detected in the human retina a major IGF-I mRNA transcript of the expected molecular mass of 7.5 kb (Fig. 1). As noted in previous studies (21), the intensity of the β-actin signal was similar in the retinas of diabetic and nondiabetic donors (3,174 ± 794 vs. 3,387 ± 1,032 densitometric units, respectively, P = 0.7), and it was thus used as internal standard. In the diabetic retinas, the levels of IGF-I mRNA were significantly decreased compared with the nondiabetic controls (IGF-I–to–β-actin ratio: 0.017 ± 0.010 vs. 0.050 ± 0.021, respectively; P = 0.005). No correlations were found in diabetic or nondiabetic donors between IGF-I mRNA levels and time to the eyes' enucleation or processing, nor with duration of diabetes in diabetic donors. The stability of the IGF-I transcript in the postmortem period was verified in rat retinas. The IGF-I– to–β-actin ratio—measured by C-RT-PCR—in rat retinas processed 27 h after the time the rats were killed was 98 ± 14% of the ratio recorded in retinas processed immediately.

To confirm the observations made in the human retinas and obtain time-course data, we studied the expression of IGF-I in the retina of diabetic and galactose-fed rats after 2 and 5 months of diabetes or galactose feeding. Because the yield of RNA from individual rat retinas was not sufficient to perform Northern blotting, the levels of IGF-I mRNA were measured by C-RT-PCR. The IGF-I primers were designed to amplify both the IGF-Ia and IGF-Ib alternatively spliced forms of the IGF-I transcript; however, only IGF-Ia was detected in rat retina (and brain) using our conditions. The characteristics

TABLE 2
Characteristics of rats studied for retinal IGF-I expression and signaling

	2 Months			5 Months		
	n	Body weight (g)	HbA_{1c} (%)	*n*	Body weight (g)	HbA_{1c} (%)
Control	5	492 ± 17	4.3 ± 0.6	8	626 ± 62	3.8 ± 0.2
Diabetic	5	285 ± 32*	11.5 ± 2.2*	7	361 ± 51*	12.0 ± 0.9*
Galactosemic	4	417 ± 41†‡	6.4 ± 0.7†‡	4	530 ± 35†‡	5.9 ± 0.4*‡

Data are means ± SD. *P < 0.0001 vs. control; †P < 0.05 vs. control; ‡P < 0.003 vs. diabetic.

of the rats are reported in Table 2. After 2 months of diabetes, body weight was significantly lower and HbA_{1c} levels significantly higher in diabetic than in control rats, but retinal expression of IGF-I was practically identical in the two groups (IGF-I–to–β-actin ratios 0.011 ± 0.011 and 0.011 ± 0.007, respectively) (Fig. 2). In the diabetic as well as the control rats killed at 5 months, body weight was 27% higher than the value recorded in the respective group at 2 months; however, IGF-I mRNA levels were now different. The IGF-I–to–β-actin ratio had increased in the control rats to 0.022 ± 0.007, but remained 0.013 ± 0.006 in the diabetic rats (P < 0.02 vs. age-matched controls) (Fig. 2). At both 2 and 5 months, the body weight and HbA_{1c} levels of galactose-fed rats were intermediate between those of diabetic and control rats (Table 2), and the IGF-I mRNA levels were not significantly different from those of controls (Fig. 2). Because the β-actin mRNA levels showed large variations among animals, the experiments were repeated using cyclophilin as the internal standard to control for input RNA. In the 19 samples tested at the 5-month time point, the cyclophilin mRNA levels correlated with those of β-actin (r = 0.6, P = 0.006) and the IGF-I–to–cyclophilin ratios yielded the same pattern of results as the IGF-I–to–β-actin ratios. Cyclophilin was used in all successive C-RT-PCR assays.

Retinal IGF-I expression is growth-hormone independent. In streptozotocin-induced diabetic rats, growth-hormone levels as well as growth-hormone receptors have been reported to be low (14). To evaluate the relevance of these abnormalities to the decreased retinal IGF-I levels, we tested whether IGF-I synthesis in the retina is regulated by growth hormone. Hypophysectomized and sham-operated control rats were compared vis-à-vis the levels of IGF-I mRNA in the liver, brain, and retina. In the liver, in which IGF-I synthesis is known to be growth-hormone dependent, IGF-I mRNA levels were significantly decreased in the hypophysectomized rats compared with the controls (IGF-I–to–cyclophilin ratio 5.2 ± 1.7 vs. 14.2 ± 4.2, P = 0.02) (Fig. 3). In contrast, in the brain, in

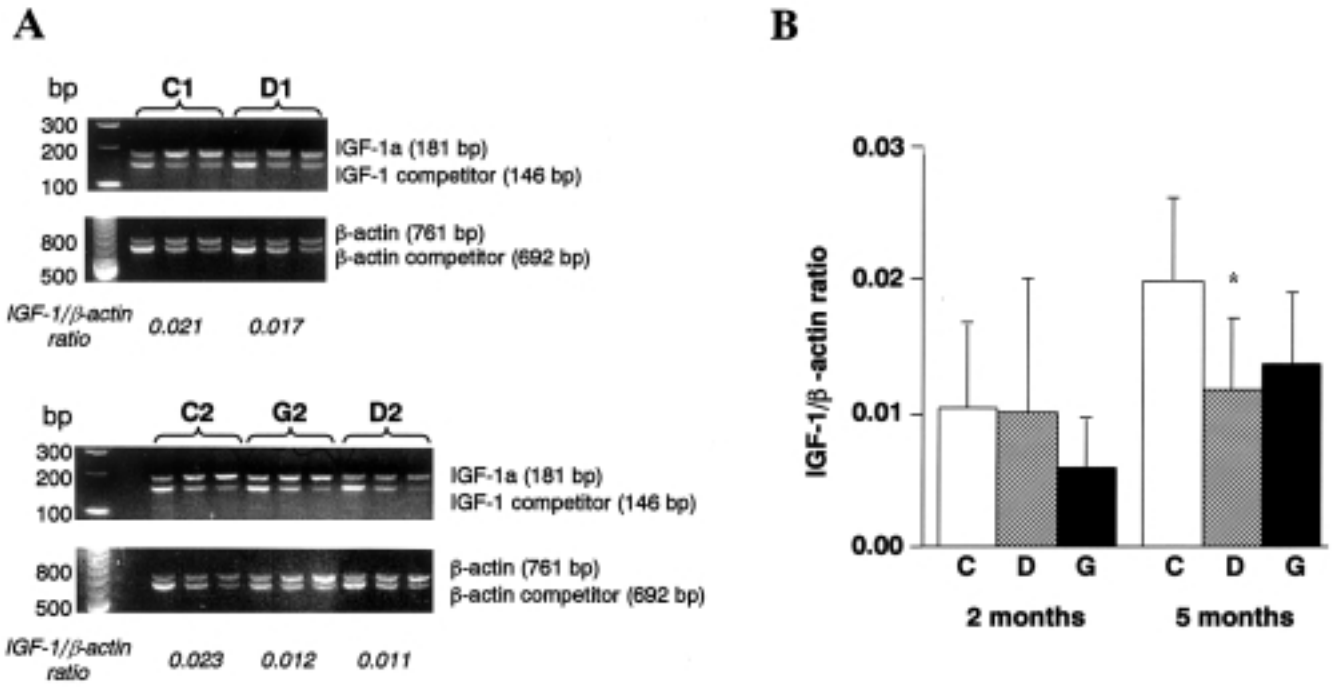

FIG. 2. IGF-I mRNA levels in the retina of diabetic and galactosemic rats. C-RT-PCR was performed as described in RESEARCH DESIGN AND METHODS using β-actin as the housekeeping gene. *A*: GelStar-stained gels showing the PCR products from two control rats (C1, C2), two rats with 5 months' diabetes duration (D1, D2), and one rat with 5 months of galactosemia (G2). Each PCR reaction was carried out in triplicate using 0.08, 0.04, and 0.02 amol IGF-I competitor, and 8, 4, and 2 amol β-actin competitor. The first lane on the left carries molecular weight standards. *B*: The amount of endogenous transcript was calculated as described in RESEARCH DESIGN AND METHODS, and data are expressed as IGF-I–to–β-actin ratio. Bars represent the mean ± SD of the values obtained in the animals described in Table 2. C, control rats; D, diabetic rats; G, galactosemic rats. *P = 0.02 vs. control.

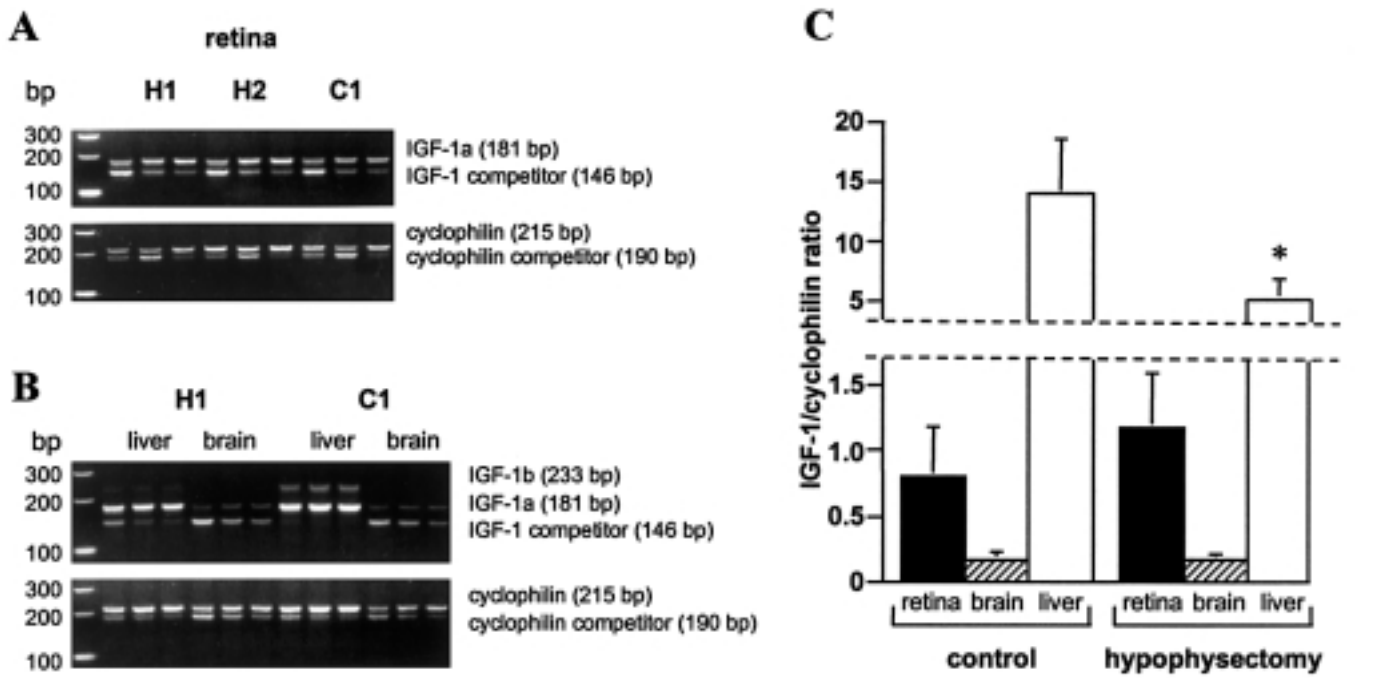

FIG. 3. IGF-I expression in the retina, brain, and liver of hypophysectomized and control rats. C-RT-PCR was performed as described in RESEARCH DESIGN AND METHODS using cyclophilin as the housekeeping gene. *A*: GelStar-stained gel showing the PCR products from the retina of two hypophysectomized (H1, H2) rats and one control (C1) rat. Each PCR reaction was carried out in triplicate using 0.08, 0.04, and 0.02 amol IGF-I and cyclophilin competitor. The first lane on the left carries molecular weight standards. *B*: Analysis of the corresponding liver and brain mRNAs. In the liver, the IGF-Ib transcript also was detected. *C*: The amount of the endogenous transcript was calculated as described in RESEARCH DESIGN AND METHODS, and data are expressed as IGF-I–to–cyclophilin ratio. Bars represent the mean ± SD of the values obtained in three controls and three hypophysectomized rats. *P = 0.02.

which IGF-I levels have been reported to be growth-hormone independent (25), the IGF-I–to–cyclophilin ratio was similar in hypophysectomized (0.2 ± 0.02) and control (0.2 ± 0.06) rats. The retina behaved like the brain, showing IGF-I mRNA levels clearly unaffected by hypophysectomy (IGF-I–to–cyclophilin ratio 1.0 ± 0.3 vs. 0.6 ± 0.2 in control rats) and indicating that retinal IGF-I levels are growth-hormone independent.

The IGF-IR is abundantly expressed in the retina and modestly increased in human diabetes. Immunoblot analysis of human and rat tissues showed that the two IGF-IR subunits are more abundant in the retina than in the brain, heart, or kidney (Fig. 4*A*). A larger species of ~180 kDa, most likely representing the IGF-IR precursor, was visible in both the retina and brain, and especially prominent in the rat. The human retinal IGF-IR α-subunit (Fig. 4*B*) was noted to migrate as a doublet, with the smaller-size species migrating in parallel with the brain α-subunit and the larger-size species with the α-subunit of the isolated retinal microvasculature. Because the larger-size band reflects mostly the contribution of IGF-IR in retinal vessels and glia, it indicates an especially prominent representation of IGF-IR on nonneuronal structures in the retina.

In the retinas of 10 diabetic human donors, the levels of the IGF-IR α- and β-subunits (137 ± 22 and 120 ± 23 densitometric units/μg protein, respectively) were greater than in nondiabetic donors (120 ± 24 and 98 ± 19 densitometric units/μg protein, respectively; P = 0.02). The measurements of the α- and β-subunits showed excellent correlation in individual samples (r = 0.8, P < 0.0001) and reproducibility in different assays (coefficient of variation 14 ± 4% for the seven retinal lysates tested in three or more assays). Rat experiments showed that the levels of the retinal IGF-IR are not affected by the postmortem period (the IGF-IR β-subunit levels in retinas processed 27 h after the time the animals were killed were 97% of levels in retinas processed immediately).

In the retinas of the same diabetic and galactosemic rats tested for IGF-I expression, the levels of the IGF-IR α-subunit were not different from those recorded in control rats (77 ± 22 densitometric units/μg protein in diabetic rats, 84 ± 22 in galactosemic rats, and 72 ± 13 in controls at the 2-month time point; and 93 ± 12, 88 ± 17, and 88 ± 8 in the corresponding groups studied at the 5-month time point).

Phosphorylation of IGF-IR and Akt are not decreased in the retina of diabetic rats. We tested whether the decreased levels of endogenous IGF-I observed in diabetic retinas resulted in compromised activation of the IGF-IR. Tyrosine-phosphorylated IGF-IR β-subunit was positively identified in cultured fibroblasts treated with IGF-I and was clearly detected in the normal rat retina (Fig. 5*A*). Detection was dependent on immediate processing of the tissue, as shown by the complete absence of the band reacting with antiphosphotyrosine antibodies in rat retinas stored for 24 h as well as human postmortem retinas (Fig. 5*B*). Phosphorylation of the IGF-IR β-subunit in the rat retina was not altered by 5 months of diabetes (94 ± 18% of control values) or galactosemia (82 ± 8% of control) (Fig. 6). To confirm this result at a functional level, we evaluated in the same retinas the phosphorylation status of Akt, a downstream target of IGF-IR signaling. The level of retinal Akt phosphorylation was not altered in the diabetic rats (123 ± 21% of control; P = 0.07) and was slightly increased in the galactosemic rats (132 ± 14% of control; P = 0.02) (Fig. 7).

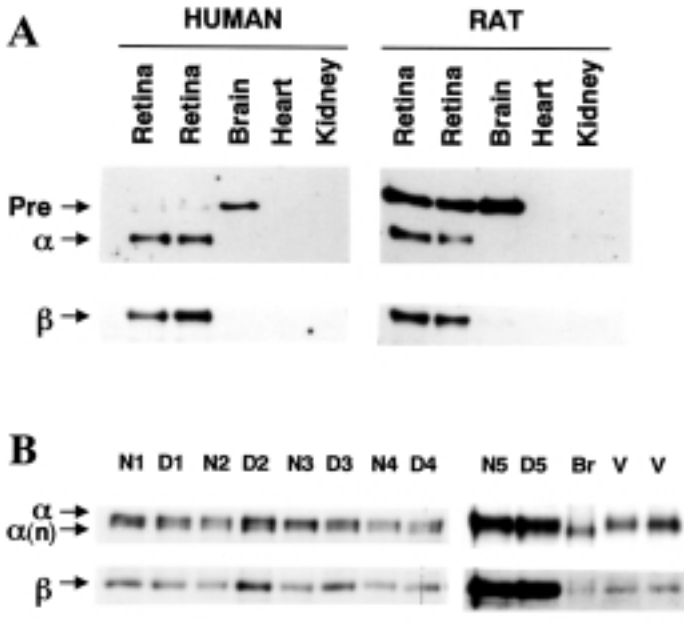

FIG. 4. IGF-IR in the retina. ***A*****: Human and rat whole-tissue lysates (40 µg per lane) were resolved by SDS-PAGE and electroblotted to nitrocellulose membranes. Blots were probed sequentially with anti–IGF-IR α-subunit polyclonal antibodies (upper panel), and anti–IGF-IR β-subunit (lower panel) polyclonal antibodies. Pre, IGF-IR precursor.** ***B*****: Retinal lysates (40 µg per lane) from five diabetic (D1–D5) donors and five age-matched nondiabetic (N1–N5) donors were studied by immunoblot as described in (*A*). Br, human brain (40 µg); V, human retinal vessels (20 µg). α(n) = IGF-IR α-subunit neuronal subtype.**

Reduced retinal IGF-I expression in diabetic rats is not accompanied by capillary cell apoptosis. The studies of IGF-I signaling performed in total retinal tissue might not have informed adequately about IGF-I signaling to discrete cell populations. Retinal capillary cell apoptosis was thus examined, to determine possible consequences of reduced IGF-I synthesis at the level of the microvasculature. The characteristics of the rats used in these experiments were identical to those reported in Table 2 for companion rats in the respective groups. Only an occasional TUNEL-positive cell was observed in the capillaries of control rats (Table 3), in accordance with our previous findings in a different cohort (1). Two or five months of diabetes did not increase the frequency of capillary cell apoptosis; 5 months of galactosemia, however, resulted in a significant number of TUNEL-positive microvascular cells ($P = 0.01$ vs. age-matched control and diabetic rats).

DISCUSSION

We examined in this study whether diabetes leads to decreased IGF-I mRNA levels in the retina, as it does in many other tissues (13–16), and whether decreased IGF-I synthesis generated a proapoptotic environment. Although we observed that the retinal synthesis of this powerful survival factor is decreased in both human and experimental diabetes, we did not detect changes in the activation of its receptor and phosphorylation of a downstream antiapoptotic effector, nor a temporal relationship between decreased IGF-I synthesis and occurrence of retinal microvascular cell apoptosis.

Decreased IGF-I synthesis appears to be an early feature of diabetic retinopathy, but not an immediate counterpart of insulin deficiency, stunted growth, or defective growth-hormone signaling. The eye donors had a short duration of type 2 diabetes. Even if duration had been longer than declared because of the extended asymptomatic period in this type of diabetes, our previous studies had shown in donors with similar characteristics: only incipient retinal microangiopathy and no proliferative changes (1,26). The diabetes-induced suppression of IGF-I synthesis has a degree of selectivity, because the human diabetic retinas with almost undetectable IGF-I mRNA had shown in a previous study unaltered levels of vascular endothelial growth factor mRNA (21). Insulin deficiency is not prominent in type 2 diabetes, but was present to a degree in the streptozotocin-induced diabetic rats that required insulin to prevent catabolism. Yet during the first 2 months of diabetes, which was also the time of a profound growth delay, retinal IGF-I mRNA levels remained similar to control values. The regulation of retinal IGF-I changed, however, between the second and fifth month of study, and the diabetic rats failed to increase IGF-I mRNA despite a percent increase in body weight similar to control rats during this period. Low levels of serum

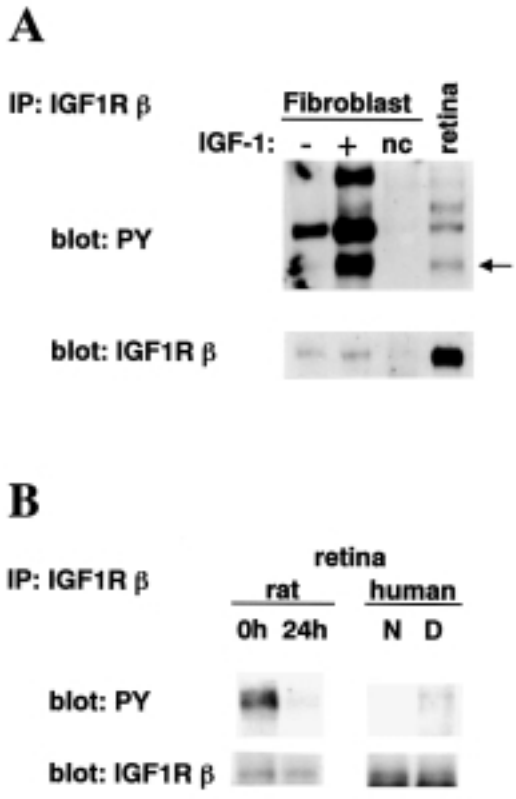

FIG. 5. Detection of IGF-IR tyrosine phosphorylation in rat retina. ***A*****: Lysates of cultured human skin fibroblasts or rat retina were immunoprecipitated with polyclonal antibodies against the IGF-IR β-subunit, resolved by SDS-PAGE, and electroblotted to nitrocellulose membranes. Blots were probed with phosphotyrosine antibody (PY, upper panel), or with IGF-IR β-subunit antibodies (IGF-IRβ, lower panel), to control for the amount of immunoprecipitated receptor. Fibroblasts incubated with (+) or without (–) IGF-I were used to positively identify the band corresponding to the tyrosine-phosphorylated IGF-IR β-subunit (←). nc, Negative control (lysate of IGF-I–treated fibroblasts immunoprecipitated with preimmune rabbit IgGs).** ***B*****: Rat retinas were processed immediately (0 h) or 24 h after the animals were killed to mimic the processing time of the human specimens. N, retinal lysates from a nondiabetic donor; D, retinal lysates from an age-matched diabetic donor.**

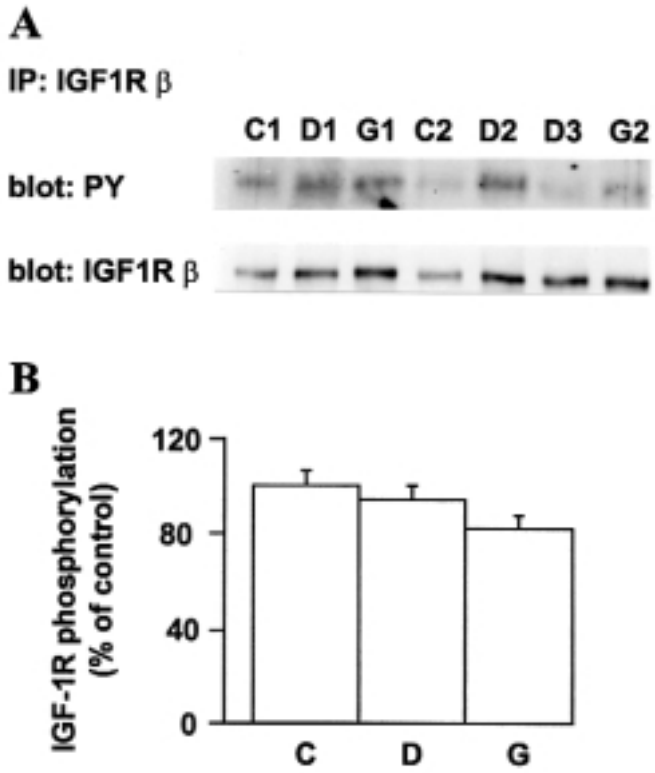

FIG. 6. IGF-IR phosphorylation in the retina of diabetic and galactosemic rats. *A*: Retinal lysates were immunoprecipitated, blotted, and probed as described in the legend of Fig. 5. *B*: Bands corresponding to the phosphorylated and total IGF-IR β-subunit (95 kDa) were quantitated by laser densitometry; their ratio was calculated, and expressed as percentage of control. Bars represent the mean ± SD of the values obtained in control (C) (n = 5), diabetic (D) (n = 5), and galactosemic (G) (n = 4) rats.

growth-hormone characteristic of aging (27) and streptozotocin-induced diabetes (14) cannot account for the reduced IGF-I synthesis in the diabetic retina, because the diabetic and nondiabetic eye donors were perfectly matched for age, and retinal IGF-I synthesis was found to be growth-hormone independent, akin to brain IGF-I (25). The retina and the brain may have in place unique mechanisms for IGF-I regulation to compensate for the limited transfer of circulating growth hormone across the blood-retinal and blood-brain barriers (28). Such uniqueness will make it more interesting to reconstruct how diabetes reduces endogenous IGF-I synthesis in these organs. A direct contribution of hyperglycemia is currently uncertain. The isolated hyperhexosemia achieved in the galactose-fed rats was insufficient to fully mimic the effects of diabetes, but it was also of a much lesser degree than diabetic hyperglycemia, as indicated by the lower HbA_{1c} levels in galactosemic as compared with diabetic rats.

To ascertain whether lower retinal IGF-I synthesis in diabetes could be expected to result in decreased signaling, we measured levels of receptor and receptor phosphorylation. The human diabetic retinas showed a small increase in IGF-IR levels when compared with nondiabetic specimens, and no change was observed in the diabetic rat retina, reflecting the inconsistent pattern of IGF-IR variations in diabetic tissues showing decreased expression of IGF-I (13,16). IGF-IR phosphorylation could be measured only in the rat retina, and the levels were not affected by diabetes, suggesting that either the degree of reduction in IGF-I synthesis was insufficient to compromise receptor activation, or that changes had occurred in other modulatory influences. One such change could be increased retinal synthesis of IGF-II, which binds the IGF-IR with slightly lower affinity than IGF-I (13). The observation, however, that IGF-II mRNA levels are substantially decreased in the brain of diabetic rats (29) does not favor this possibility. A role could be played by increased availability of IGF-I and/or IGF-II derived from the circulation. Just as circulating IGFs can cross the capillary barrier in selected areas of the brain (30), they may cross the capillary barrier in the retina; and if this barrier is compromised by diabetes, larger amounts of IGFs may reach the retinal tissue. We could not perform measurements to test this possibility, because our rats were not perfused at the time of killing, and therefore retinal IGFs levels would have reflected an unknown contribution from IGFs in trapped blood. On the other hand, recent evidence suggests that endocrine-acting IGF-I is less important than locally produced IGF-I in tissue signaling and action (31). The activity of the IGF-IR can also be modulated by IGF-I–binding proteins, which can either enhance or reduce IGF-I availability to its receptor (13), and the levels of several of these proteins change in diabetes (13). The difficulty in testing the role of any such change is that the affinity of protein binding to IGF-I and

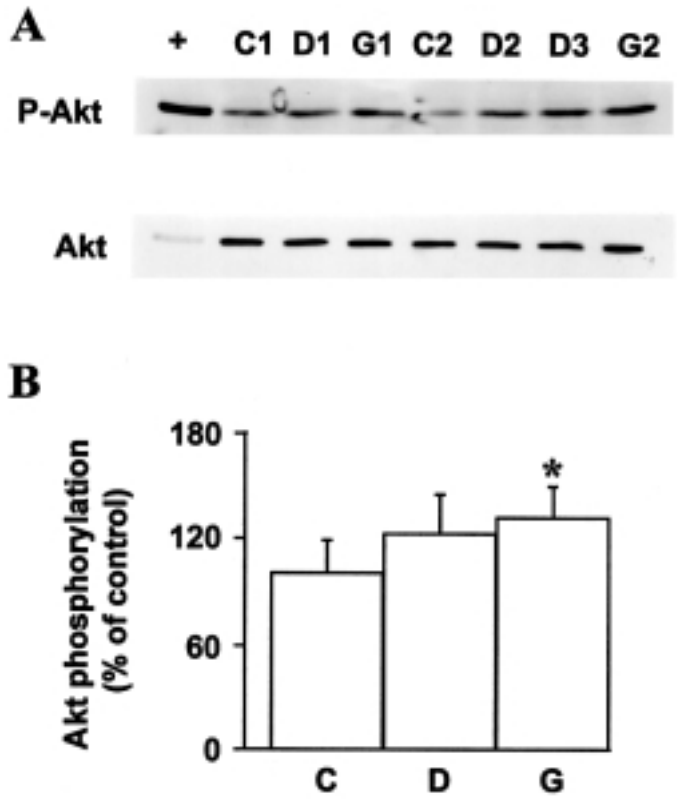

FIG. 7. Akt phosphorylation in the retina of diabetic and galactosemic rats. *A*: Retinal lysates (50 µg per lane) were resolved by SDS-PAGE and electroblotted to nitrocellulose membrane. Blots were probed with antiphosphorylated Akt (P-Akt, upper panel) or anti–Akt antibodies (lower panel) to control for the amount of Akt. (+), Positive control (lysate of platelet-derived growth factor–treated endothelial cells). *B*: Bands were quantitated by laser densitometry; their ratio calculated, and expressed as percentage of control. Bars represent the mean ± SD of the values obtained in control (C) (n = 5), diabetic (D) (n = 5), and galactosemic (G) (n = 4) rats. *P = 0.02 vs. control.

TABLE 3
TUNEL-positive capillary cells in the retinas of diabetic and galactosemic rats

	2 Months				5 Months			
	P	E	UD	Total	P	E	UD	Total
Control	0.2 ± 0.4	0.2 ± 0.4	0.2 ± 0.4	0.6 ± 0.9	0.2 ± 0.4	0.2 ± 0.4	0.2 ± 0.4	0.6 ± 0.9
Diabetic	0	0.6 ± 0.5	1.0 ± 0.7	1.6 ± 0.9	0.2 ± 0.4	0.4 ± 0.5	0	0.6 ± 0.9
Galactosemic	0.3 ± 0.5	0.8 ± 0.9	0.8 ± 0.9	1.8 ± 1.7	3.2 ± 1.6	0.8 ± 0.8	1.0 ± 1.0	5.0 ± 2.8*

Data are means ± SD of the TUNEL-positive cells counted in each retina. E, endothelial cell; P, pericyte; UD, undetermined cell type (the size, shape, or topography of the positive chromatin did not permit attribution to pericytes or endothelial cells). $n = 5$ in each group, at each time point. *$P = 0.01$ vs. control.

the functional outcome are often dependent on posttranslational events (13) that cannot be predicted from protein abundance.

Further verification that basal IGF-I signaling was not compromised in the diabetic rat retina was provided by the finding that Akt phosphorylation was not decreased, and actually tended to be enhanced. This is noteworthy, because Akt phosphorylation is downstream not only of the IGF-IR, but also of the insulin receptor (9,32), and the diabetic rats in this study had systemic signs of chronic insulin deficiency and received no insulin replacement for at least 48 h before they were killed. This raises the possibility that Akt regulation in the retina is not responsive to circulating insulin levels, or, as proposed earlier for IGF-I, that the degree of ligand deficiency is not sufficient to compromise signaling or is compensated for by other local influences. A modest but significant increase over control was found in the levels of Akt phosphorylation in the retina of galactosemic rats, which also showed increased frequency of capillary cell apoptosis. Akt phosphorylation may reflect in these retinas the contribution of cellular stress, which can induce Akt activation through the p38/HOG1 kinase cascade (32,33). The earlier onset of retinal capillary cell apoptosis in the galactosemic than diabetic rats is in accord with our previous findings that rats with 6-month duration of galactosemia showed a significant number of acellular capillaries not noted in rats with almost 8 months of diabetes (1). The different time of onset of vascular apoptosis in diabetic and galactosemic rats, coupled with the selective effect of aminoguanidine on diabetes-induced apoptosis and retinopathy (34), indicates that different mechanisms initiate the pathway to retinal microangiopathy in the two models. Apoptosis of retinal neurons was not examined in this study, but the timing of occurrence reported by Barber et al. (4)—as early as 1 month after induction of streptozotocin diabetes in the rat—militates against a contribution from decreased IGF-I synthesis, which was as yet unaltered after 2 months of experimental diabetes.

Although a multitude of studies have investigated IGF-I in diabetic tissues and found decreased synthesis, signaling and biological consequences have largely been surmised. This work shows that reduced IGF-I mRNA levels in diabetes do not necessarily translate into decreased biological actions, at least for some time, and perhaps on account of modulatory/compensatory influences. However, IGF-I signaling could only be studied in the rat retina, and diabetic rats had shown a lesser degree of suppression of retinal IGF-I synthesis than the human diabetic donors. Hence, our data cannot exclude consequences of the more severe changes observed in human diabetes, nor can they exclude that treatment with exogenous IGF-I may have beneficial effects on the course of diabetic retinopathy. However, the data warn that exogenous IGF-I would represent a pharmacological intervention rather than necessary replacement until proof is obtained that decreased retinal IGF-I synthesis in diabetes is a primary defect (and not, for example, the result of processes that modulate IGF-I affinity for its receptor), and plays a pathogenic role in the development of retinopathy.

ACKNOWLEDGMENTS

This work was supported by Public Health Service Grant EY09122, a grant from the Massachusetts Lions Eye Research Fund, and the George and Frances Levin Endowment. G.R. was the recipient of a fellowship from the board of trustees of the Schepens Eye Research Institute.

We are indebted to Dr. A. Kazlauskas for the gift of platelet-derived growth factor–treated endothelial cells and for critical reading of the manuscript.

REFERENCES

1. Mizutani M, Kern TS, Lorenzi M: Accelerated death of retinal microvascular cells in human and experimental diabetic retinopathy. *J Clin Invest* 97:2883–2890, 1996
2. Li W, Yanoff M, Jian B, He Z: Altered mRNA levels of antioxidant enzymes in pre-apoptotic pericytes from human diabetic retinas. *Cell Mol Biol* 45:59–66, 1999
3. Podestà F, Romeo G, Liu W-H, Krajewski S, Reed JC, Gerhardinger C, Lorenzi M: Bax is increased in the retina of diabetic subjects and is associated with pericyte apoptosis in vivo and in vitro. *Am J Pathol* 156:1025–1032, 2000
4. Barber AJ, Lieth E, Khin SA, Antonetti DA, Buchanan AG, Gardner TW: Neural apoptosis in the retina during experimental and human diabetes: early onset and effect of insulin. *J Clin Invest* 102:783–791, 1998
5. Waldbillig RJ, Fletcher RT, Somers RL, Chader GJ: IGF-I receptors in the bovine neural retina: structure, kinase activity and comparison with retinal insulin receptors. *Exp Eye Res* 47:587–607, 1988
6. Burren CP, Berka JL, Edmondson SR, Werther GA, Batch JA: Localization of mRNAs for insulin-like growth factor-I (IGF-I), IGF-I receptor, and IGF binding proteins in rat eye. *Invest Ophthalmol Vis Sci* 37:1459–1468, 1996
7. Moriarty P, Boulton M, Dickson A, McLeod D: Production of IGF-I and IGF binding proteins by retinal cells in vitro. *Br J Ophthalmol* 78:638–642, 1994
8. King GL, Goodman AD, Buzney S, Moses A, Kahn CR: Receptors and growth-promoting effects of insulin and insulinlike growth factors on cells from bovine retinal capillaries and aorta. *J Clin Invest* 75:1028–1036, 1985
9. Peruzzi F, Prisco M, Dews M, Salomoni P, Grassilli E, Romano G, Calabretta B, Baserga R: Multiple signaling pathways of the insulin-like growth factor 1 receptor in protection from apoptosis. *Mol Cell Biol* 19:7203–7215, 1999
10. Brunet A, Bonni A, Zigmond MJ, Lin MZ, Juo P, Hu LS, Anderson MJ, Arden KC, Blenis J, Greenberg ME: Akt promotes cell survival by phosphorylating and inhibiting a forkhead transcription factor. *Cell* 96:857–868, 1999
11. Cardone MH, Roy N, Stennicke HR, Salvesen GS, Franke TF, Stanbridge E, Frisch S, Reed JC: Regulation of cell death protease caspase-9 by phosphorylation. *Science* 282:1318–1321, 1998
12. Deckwerth TL, Elliott JL, Knudson CM, Johnson EM, Snider WD, Korsmeyer SJ: BAX is required for neuronal death after trophic factor deprivation and during development. *Neuron* 17:401–411, 1996

13. Bach LA, Rechler MM: Insulin-like growth factors and diabetes. *Diabetes Metab Rev* 8:229–257, 1992
14. Fagin JA, Roberts CT Jr, LeRoith D, Brown AT: Coordinate decrease of tissue insulinlike growth factor I posttranscriptional alternative mRNA transcripts in diabetes mellitus. *Diabetes* 38:428–434, 1989
15. Ishii DN, Guertin DM, Whalen LR: Reduced insulin-like growth factor-I mRNA content in liver, adrenal glands and spinal cord of diabetic rats. *Diabetologia* 37:1073–1081, 1994
16. Busiguina S, Chowen JA, Argente J, Torres-Aleman I: Specific alterations of the insulin-like growth factor I system in the cerebellum of diabetic rats. *Endocrinology* 137:4980–4987, 1996
17. Lowe WL, Florkiewicz RZ, Yorek MA, Spanheimer RG, Albrecht BN: Regulation of growth factor mRNA levels in the eye of diabetic rats. *Metabolism* 44:1038–1045, 1995
18. Charkrabarti S, Ghahary A, Murphy LJ, Sima AAF: Insulin-like growth factor-I expression is not increased in the retina of diabetic BB/W-rats. *Diabetes Res Clin Pract* 14:91–98, 1991
19. LeRoith D, Werner H, Beitner-Johnson D, Roberts CT: Molecular and cellular aspects of the insulin-like growth factor I receptor. *Endocrine Rev* 16:143–163, 1995
20. Engerman RL, Kern TS: Retinopathy in animal models of diabetes. *Diabetes Metab Rev* 11:109–120, 1995
21. Gerhardinger C, Brown LF, Roy S, Mizutani M, Zucker CL, Lorenzi M: Expression of vascular endothelial growth factor in the human retina and in nonproliferative diabetic retinopathy. *Am J Pathol* 152:1453–1462, 1998
22. Celi FS, Zenilman ME, Shuldiner AR: A rapid and versatile method to synthesize internal standards for competitive PCR. *Nucleic Acids Res* 21:1047, 1993
23. Vafiadis P, Grabs R, Goodyer CG, Colle E, Polychronakos C: A functional analysis of the role of *IGF2* in *IDDM2*-encoded susceptibility to type 1 diabetes. *Diabetes* 47:831–836, 1998
24. Mizutani M, Gerhardinger C, Lorenzi M: Müller cell changes in human diabetic retinopathy. *Diabetes* 47:445–449, 1998
25. D'Ercole AJ, Stiles AD, Underwood LE: Tissue concentrations of somatomedin C: further evidence for multiple sites of synthesis and paracrine or autocrine mechanisms of action. *Proc Natl Acad Sci U S A* 81:935–939, 1984
26. Roth T, Podestà F, Stepp MA, Boeri D, Lorenzi M: Integrin overexpression induced by high glucose and by human diabetes: potential pathway to cell dysfunction in diabetic microangiopathy. *Proc Natl Acad Sci U S A* 90:9640–9644, 1993
27. Finkelstein JW, Roffwarg HP, Boyar RM, Kream J, Hellman L: Age-related change in the twenty-four-hour spontaneous secretion of growth hormone. *J Clin Endocrinol Metab* 35:665–670, 1972
28. Prahalada S, Block G, Handt L, DeBurlet G, Cahill M, Hoe CM, van Zwieten MJ: Insulin-like growth factor-1 and growth hormone (GH) levels in canine cerebrospinal fluid are unaffected by GH or GH secretagogue (MK-0677) administration. *Horm Metab Res* 31:133–137, 1999
29. Wuarin L, Namdev R, Burns JG, Fei ZJ, Ishii DN: Brain insulin-like growth factor-II mRNA content is reduced in insulin-dependent and non-insulin-dependent diabetes mellitus. *J Neurochem* 67:742–751, 1996
30. Reinhardt RR, Bondy CA: Insulin-like growth factors cross the blood-brain barrier. *Endocrinology* 135:1753–1761, 1994
31. Sjögren K, Liu JL, Blad K, Skrtic S, Vidal O, Wallenius V, LeRoith D, Törnell J, Isaksson OGP, Jansson JO, Ohlsson C: Liver-derived insulin-like growth factor I (IGF-I) is the principal source of IGF-I in blood, but is not required for postnatal body growth in mice. *Proc Natl Acad Sci U S A* 96:7088–7092, 1999
32. Downward J: Mechanisms and consequences of activation of protein kinase B/Akt. *Curr Opin Cell Biol* 10:262–267, 1998
33. Konishi H, Matsuzaki H, Tanaka M, Ono Y, Tokunaga C, Kuroda S, Kikkawa U: Activation of RAC-protein kinase by heat shock and hyperosmolarity stress through a pathway independent of phosphatidylinositol 3-kinase. *Proc Natl Acad Sci U S A* 93:7639–7643, 1996
34. Kern TS, Tang J, Mizutani M, Kowluru R, Nagaraj R, Romeo G, Podestà F, Lorenzi M: Response of capillary cell death to aminoguanidine predicts the development of retinopathy: comparison of diabetes and galactosemia. *Invest Ophthalmol Vis Sci* 41:3972–3978, 2000